7-18-1995

The kinetics of quantal transmitter release from retinal amacrine cells

Salvador Borges
University of California, Davis

Evanna Gleason
University of California, Davis

Michael Turelli
University of California, Davis

Martin Wilson
University of California, Davis

Recommended Citation

Borges, S., Gleason, E., Turelli, M., & Wilson, M. (1995). The kinetics of quantal transmitter release from retinal amacrine cells. *Proceedings of the National Academy of Sciences of the United States of America, 92* (15), 6896-6900. https://doi.org/10.1073/pnas.92.15.6896

Proc. Natl. Acad. Sci. USA
Vol. 92, pp. 6896–6900, July 1995
Neurobiology

The kinetics of quantal transmitter release from retinal amacrine cells

(synapse/calcium/exocytosis)

SALVADOR BORGES*, EVANNA GLEASON*†, MICHAEL TURELLI‡, AND MARTIN WILSON*§

*Section of Neurobiology, Physiology, and Behavior and ‡Section of Evolution and Ecology, Division of Biological Sciences, University of California, Davis, CA 95616

Communicated by Peter Marler, University of California, Davis, CA, April 24, 1995

ABSTRACT **Exocytosis of transmitter at most synapses is a very fast process triggered by the entry of Ca^{2+} during an action potential. A reasonable expectation is that the fast step of exocytosis is followed by slow steps readying another vesicle for exocytosis but the identity and kinetics of these steps are presently unclear. By voltage clamping both pre- and postsynaptic neurons in an isolated pair of retinal amacrine cells, we have measured evoked synaptic currents and responses to single vesicles of transmitter (minis). From these currents, we have computed the rate of exocytosis during a sustained presynaptic depolarization. We show here that for these cells, release is consistent with a scheme of "fire and reload." Large Ca^{2+} influx causes the rapid release of a small number of vesicles, typically ≈10 per presynaptic neuron, likely corresponding to those vesicles already docked. After this spike of exocytosis whose peak is 150 quanta per release site per s, continued Ca^{2+} influx sustains release at only 22 quanta per release site per s, probably rate-limited by the docking of fresh vesicles.**

A critical distinction between different models of transmitter release lies in the rate at which vesicles of transmitter are exocytosed (1). Release rates from nonneuronal secretory cells (2–5) and neurons (6–9) have been measured by monitoring the increase in cell capacitance consequent upon fusion of vesicle membrane with the plasmalemma. A limitation imposed by the tiny capacitance of a transmitter vesicle is that, for ordinary neurons, single exocytic events are well below the limit of resolution. Conventional electrophysiological recording can detect single exocytic events as "miniature" currents or voltages (10, 11), but in general, synaptic current is not directly related to release rate since at any point it depends on the history of release up to that point. A way of estimating release rate while still exploiting the good resolution of synaptic current recording comes from considering synaptic current as the convolution (12) of mini waveform with the release rate (13, 14). Finding the release rate is then a matter of finding the deconvolution of these two measurable functions, the mini current time course and the evoked synaptic current time course.

METHODS

GABAergic cells (GABA, γ-aminobutyric acid) derived from embryonic chicken retina were cultured at very low density and identified as described elsewhere (15, 16). Pairs of amacrine cells having short thick dendrites and without contact to other cells were examined on embryonic equivalent days 15 through 17. Both cells were whole-cell patch-clamped by using the perforated patched method with nystatin (15, 17). The direction of strongest transmission designated the identity of the pre- and postsynaptic partners. Presynaptic cells were held at −70 mV and postsynaptic cells were held at 0 mV, positive to the calculated chloride equilibrium potential E_{Cl} (−70 mV), making the postsynaptic type A γ-aminobutyric acid receptor ($GABA_A$) currents outward. Solutions used were as follows: pipet, 135.0 mM cesium acetate/5.0 mM CsCl/2.0 mM $MgCl_2$/0.1 mM $CaCl_2$/1.1 mM EGTA/10.0 mM Hepes, pH 7.4; external, 116.9 mM NaCl/5.3 mM KCl/20.0 mM tetraethylammonium chloride/3.0 mM $CaCl_2$/0.41 mM $MgCl_2$/5.6 mM glucose/3.0 mM Hepes/300 nM tetrodotoxin, pH 7.4. In some experiments, KCl was replaced with equimolar NaCl. In these solutions, Na^+ and K^+ currents were suppressed. Cable calculations and experimental data (15, 17) suggest that pre- and postsynaptic space clamp was adequate. Clamp speed, though slow (typically τ_{clamp} = 0.8 ms) due to series resistance (R_S) values typically ≈50 MΩ, was adequate for the events described here. Experiments using ruptured patch recording pre- and postsynaptically, in which effective R_S was <5 MΩ, gave results qualitatively similar to those shown here but failed to maintain transmission for as long as perforated patch recording. Clamp currents from Axopatch 1C and 1D amplifiers (Axon Instruments, Foster City, CA) were recorded to disc, typically at a sampling rate of 5 kHz. All experiments were done at room temperature (23–25°C).

External solutions were bath-applied by gravity-flow superfusion of the cell from a 1-mm-diameter inlet pipe positioned nearby. A reference Ag–AgCl pellet immersed in saturated 3 M KCl was connected to the culture dish via a 3 M KCl agar bridge that was positioned downstream from the cell, adjacent to an outflow siphon.

For experiments on GABA desensitization, GABA in normal external solution was ejected from a 3-μm-tip pipet by means of a 7-kPa air pressure step. Phenol red was included in the pipet solution for visualizing the ejection of the drug over the cell. To avoid the effects of leakage of the drug when not pressurized, the pipet tip was initially positioned downstream and in a different laminar plane from the cell. During drug application, the pipet tip was situated one to two cell widths away and slightly upstream from the cell. Application speeds varied considerably between cells. Minimum times for 10–90% maximal GABA response were ≈5 ms. Cells chosen for GABA application experiments were single isolated amacrine cells recorded in the ruptured patch mode by using the same solutions and with perforated patch but with the addition of 1 mM ATP in the pipet and without nystatin. Cells were usually held at 0 mV but in some experiments holding voltage was brought closer to E_{Cl} to reduce voltage errors associated with large currents.

The publication costs of this article were defrayed in part by page charge payment. This article must therefore be hereby marked "*advertisement*" in accordance with 18 U.S.C. §1734 solely to indicate this fact.

Abbreviations: GABA, γ-aminobutyric acid; $GABA_A$, type A GABA receptor.

†Present address: Department of Biology, University of California, San Diego, CA 92093.
§To whom reprint requests should be addressed at: Division of Biological Sciences, Storer Hall Site, University of California, Davis, CA 95616.

RESULTS

Measurements of Postsynaptic Currents. Isolated pairs of retinal amacrine cells in sparse culture were voltage-clamped by using the perforated patch method (18). External tetrodotoxin and internal Cs^+ were employed to block Na^+ and K^+ currents. In synaptically connected pairs, activation of presynaptic Ca^{2+} current by depolarization resulted in postsynaptic current that was clearly quantal, completely blocked by Cd^{2+} or Co^{2+}, and mediated by $GABA_A$ channels (15). Ca^{2+} currents in these cells show little inactivation (decline of 17 ± 6%, mean ± SD) for steps of 100 ms (17) and evoke release (Fig. 1*A*) that continues even after the presynaptic neuron has been repolarized (15, 17) while the intracellular Ca^{2+} concentration is thought to remain high. As measured in chromaffin cells (19), $[Ca^{2+}]$ immediately under the plasmalemma is likely to be a monotonically increasing function of time during the step though $[Ca^{2+}]$ at a release site may show large temporal fluctuations due to the stochastic nature of Ca^{2+} channel opening (20). In principle, a postsynaptic current record like that in Fig. 1*A* should yield a release rate function $[r(t)]$ when deconvolved with the mini current. However, as shown in these (15) and other (21–23) neurons, minis exhibit considerable amplitude variance, which introduces uncertainty. By presuming that transmitter release sites are independent and identical, this uncertainty can be reduced by using the estimated mean evoked current $I_e(t)$ and the estimated mean mini $I_m(t)$ so that

$$I_e(t) \simeq \int_0^\infty r(t')I_m(t - t')dt'. \quad [1]$$

Minis were usually elicited by partial activation of the presynaptic Ca^{2+} current through depolarizations to approximately −35 mV, so that quanta were discretely resolvable (Fig. 1*B*). Estimates of the mean mini for each cell pair were formed by averaging between 9 and 89 well-resolved isolated minis aligned at their peaks. This average was then scaled to the mean peak amplitude derived from a larger data set of ≈250 minis. The peak amplitude for seven cells was 17.5 ± 1.75 pA (mean ± SEM). Since mini waveform is independent of amplitude (15), this scaling procedure is justified. Finally, to eliminate noise remaining in this average, piecewise analytical fits were used to generate idealized minis (Fig. 2*A*).

Means for evoked current were obtained by averaging between 10 and 21 responses time-locked to presynaptic steps to 0 mV usually of 100-ms duration. Repeated iterations of the stimulus eventually caused responses to decline, presumably as a consequence of transmitter exhaustion rather than Ca^{2+} current rundown, which was slower. Because of this decline, care was exercised to choose segments of data in which mean responses were stationary. Peak amplitudes in different pairs varied between mean values of 50.6 and 189.3 pA (Table 1). As shown in Fig. 2*B*, the peak current was followed by a decline (42 ± 16%, mean ± SD) during the 100-ms step.

Quantal Release Rates. Deconvolutions were carried out numerically as a division of the fast Fourier transform of mean evoked currents by the fast Fourier transform of the mean mini, suitably padded with zeros (MATHCAD signal processing function pack, Mathsoft, Cambridge, MA). Release rates generated this way were smoothed with a function approximating a Gaussian with an SD of 1.8 ms to eliminate spurious high-frequency oscillations including physically meaningless negative values. To check the validity of these procedures, smoothed release rates (Fig. 2*C*) were reconvolved with the average mini and the correspondence with the measured evoked current was always close (Fig. 2*B*).

The form of the release function in all seven pairs examined was like that shown in Fig. 2*C* and summarized in Table 1, in having an initial spike (mean width at half height, 7.85 ms), followed by a sustained rate, lower on average by a factor of 6.8. Smoothing of the release function necessarily broadens the width of the initial spike but experiments measuring the initial current as a function of step length (17) show that initial current continues to increase in amplitude up to step lengths of 10 ms, commensurate with the spike width described here and arguing that smoothing does not greatly distort the initial spike. Since chicken synapses are optimized for operation at 40°C but examined here at 23°C, release rates *in vivo* are likely to be much higher than those shown here since the kinetics of transmission are highly temperature-dependent (24, 25).

An obvious physical interpretation of Fig. 2*C* is that the large influx of Ca^{2+} into the presynaptic terminal causes the roughly synchronous release of vesicles from docking sites that then have to be refilled by a slower process, reloading, that is

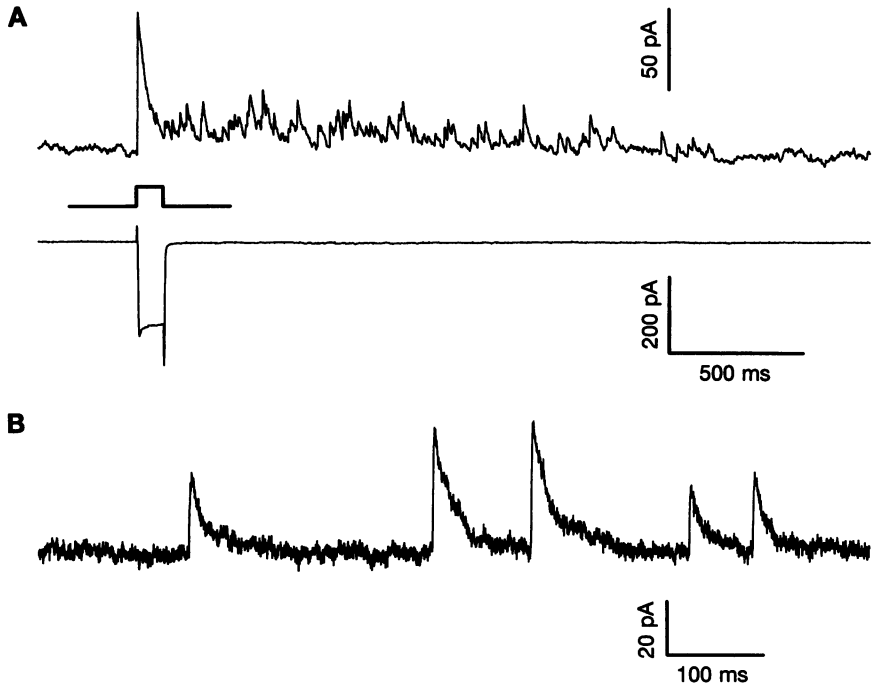

FIG. 1. Postsynaptic currents elicited by presynaptic depolarization in a pair of amacrine cells. (*A*) Simultaneously recorded pre- and postsynaptic currents (lower and upper traces, respectively) for a presynaptic step to 0 mV from −70 mV. The presynaptic Ca^{2+} current shows little inactivation during the step although postsynaptic current is distinctly transient. Transmission continues long after presynaptic repolarization and is noisy due to the quantal nature of transmission. (*B*) Continuous depolarization of a presynaptic neuron to −31 mV activates a small sustained Ca^{2+} current in the presynaptic cell (data not shown) that promotes the infrequent and random release of quanta that produce the miniature currents shown here in the postsynaptic cell.

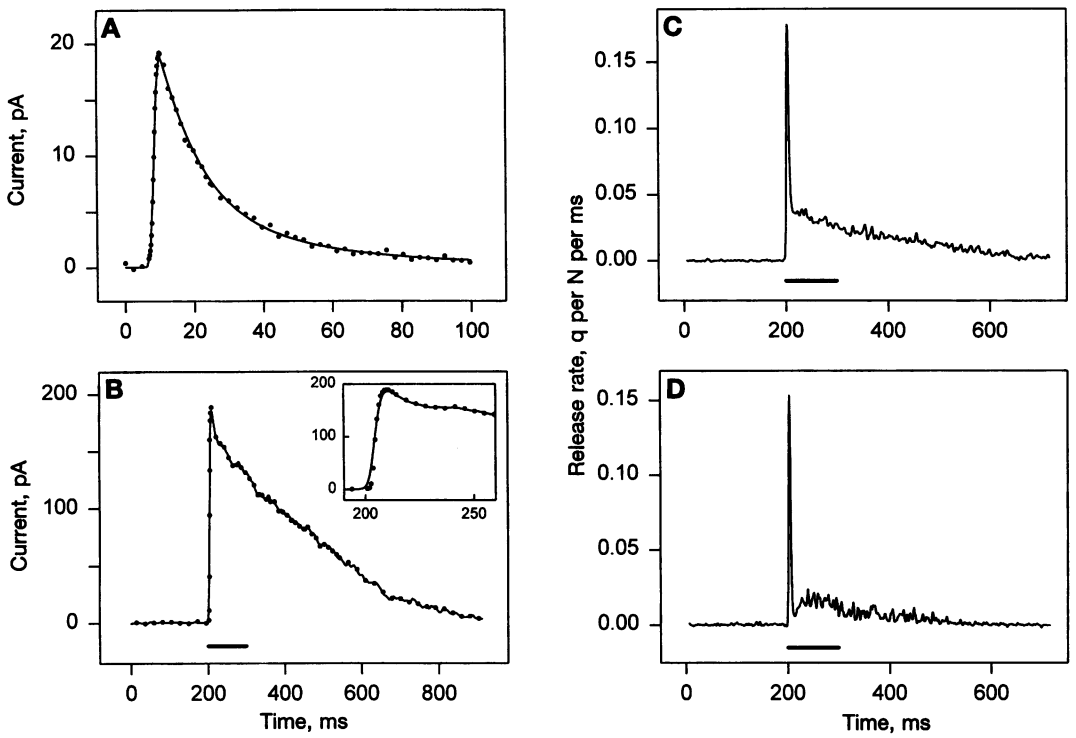

FIG. 2. Deconvolution of the mean evoked postsynaptic current and the average mini yield the quantal release rate. (*A*) Mean mini obtained by averaging 89 individual minis sampled at 5 kHz, normalized to the mean peak amplitude of 313 quanta from the same cell. An analytical description of the data points is shown as a continuous line. (*B*) For the same cell as in *A*, the mean postsynaptic current evoked by 18 iterations of a 100-ms presynaptic step to 0 mV (indicated by a bar) presented every 12 s. Currents were sampled at 5 kHz and not all data points are shown here. The continuous line is the synthesized approximation of the evoked current based on the convolution of the average mini from *A* and the computed release rate shown in *C*. (*Inset*) Rising phase of the current expanded. The continuous curve starts slightly before the data points due to the smoothing applied to the computed release rate. (*C*) Quantal release rate obtained by the deconvolution of the idealized mini response shown in *A* and the mean evoked current in *B*. Release rate is normalized to the estimated number of release sites, which in this cell was 9.75. q, Quanta; N, number of release sites. (*D*) Release rate for another cell pair in which a dip, lasting ≈20 ms, follows the initial spike.

then rate-limiting. Two out of seven cells, including the one having the narrowest initial spike, showed a noticeable dip in *r* immediately after the peak (Fig. 2*D*) that lasted ≈20 ms. Such a dip is incompatible with a simple "shot noise" model for evoked current (26), in which the reloading times are exponentially distributed. This suggests that a refractory period follows exocytosis, but establishing this hypothesis may require examination of a single release site.

Estimates of the Number of Release Sites. To normalize release rates to those at a single release site, we have estimated *N*, the number of release sites, and *p*, the probability of release, by assuming a simple binomial model of release (11, 27, 28). To do this we have used our estimates of the mean and variance of peak mini amplitudes ($I_{m,peak}$ and var $I_{m,peak}$) and formed estimates of the mean and variance of the peak evoked current ($I_{e,peak}$ and var $I_{e,peak}$) without time locking to the stimulus. *N* and *p* were found by solving the equations

$$I_{e,peak} = NpI_{m,peak} \quad [2]$$

and

$$\text{var } I_{e,peak} = I^2_{m,peak}Np(1-p) + Np \text{ var } I_{m,peak}, \quad [3]$$

where the first term in Eq. **3** is the familiar binomial term (11, 28) and the second term arises from the variance of quantal amplitude. In the seven cell pairs chosen for analysis, postsynaptic current variance not associated with transmission was

Table 1. Characteristics of transmission between seven pairs of amacrine cells

$I_{m,peak}$, pA	Step length, ms	$I_{e,peak}$, pA	*N*	*p*	Peak *r*	*r* spike half width, ms	Sustained *r*
17.4 ± 11.8	100	50.6 ± 17.4	1.99	1.19	0.17	8.34	0.030
22.3 ± 10.8	100	168.3 ± 30.3	7.63	0.99	0.15	7.37	0.020
13.4 ± 5.1	100	114.7 ± 20.2	9.69	0.88	0.07	16.7	0.021
19.2 ± 9.7	100	189.3 ± 29.8	9.75	1.01	0.18	5.83	0.031
14.7 ± 9.2	30	148.2 ± 27.6	9.67	1.04	0.16	5.99	0.020
19.5 ± 7.4	250	177.9 ± 24.4	9.37	0.97	0.20	6.40	0.017
16.2 ± 7.8	100	139.8 ± 27.3	9.52	0.90	0.15	4.30	0.017
17.5*		141.2*	8.23	1.00*	0.15*	7.85*	0.022*

N, the number of release sites, and *p*, the probability of release of a quantum contributing to the evoked current peak, were calculated from Eqs. **2** and **3**. Release rates (*r*) shown are those for the peak and the sustained rate measured 30 ms after the onset of the presynaptic step and are expressed as quanta (q) per release site per ms. The values of *N* shown in the table have been used for this normalization even though they are noninteger. Peak half width is the width of the initial release spike at its half height. $I_{m,peak}$, mean mini peak amplitude; $I_{e,peak}$, mean peak evoked response. Data for the currents are the mean ± SD.
*Mean.

small (mean = 2.5 pA^2) and has been ignored. The result of this analysis was that N was estimated to lie between 2 and 10 with a mode at 9, and p was found to be close to unity. To assess the reliability of our estimates of N and p, we performed simulations, based on measured distributions of mini amplitudes, in which N and p were varied between simulations but their product (the mean evoked response) was held constant. Solving Eqs. **2** and **3**, even for the small sample sizes used in our experiments, gave reliable estimates of both N and p when the value of p used to generate the simulated data was set at 1. If p was set at 0.9 and the number of trials to generate the mean evoked current was set at 15, the average number in our experiments, we could generate a simulated data set with which to compare p values from the seven cells in Table 1. At the 95% confidence level, the distribution of experimental p values differed (Kolmogorov–Smirnov test) from those expected if p, in all cells, was actually 0.9, or lower. An assumption in Eqs. **2** and **3** is that the initial release of transmitter is completely synchronous at all sites. The finite width of the initial spike of release (Fig. 2 *C* and *D*) suggests that this is not the case and implies, therefore, that N is somewhat underestimated in this method but corrections for asynchronous initial release were not thought worthwhile.

As a result of our estimates of N, we calculate that initial release rates per release site (Table 1) have transient values of 150 s^{-1} and sustained rates of 22 s^{-1}, indicating a mean reloading time of 45 ms.

Tests of the Deconvolution Method. A crucial assumption in estimating release rates by deconvolution is that quanta add linearly. Estimates of GABA in synaptic clefts suggest that it can briefly reach a concentration of several hundred micromolar (29). Sustained concentrations that high have been shown to cause desensitization in excised patches (29, 30) and whole cells (31), but two pieces of evidence suggest that desensitization is unlikely to account for the release kinetics found by deconvolution. (*i*) Application of GABA to amacrine cells by pressure ejection showed very little desensitization on the time scale of interest (Fig. 3*D*). For applications of 300 μM GABA, nine cells showed a mean desensitization of 2.6 ± 7.9% over 50 ms. (*ii*) In one cell pair, it was possible to estimate $r(t)$ independently of the deconvolution method. In this cell pair, synaptic exhaustion led to an effective decrease in N, the number of release sites, to ≈3, so that individual minis could be readily seen (Fig. 3*A*). Since most quanta, including those released at the beginning of a step, were not exactly synchronous, the onset of a mini in Fig. 3*A* could be detected from inspection of the time derivative of the current. Detecting the onset of minis in this way should be unaffected by desensitization and provide an estimate of $r(t)$ independent of the deconvolution method. As shown in Fig. 3*C*, the two methods give good agreement, supporting the validity of the deconvolution method and ruling out the nonlinear addition of quanta resulting from desensitization or some other cause. A qualitative confirmation of the kinetics obtained by deconvolution can be had by noticing that in the records of Fig. 3*A* and in the average shown in Fig. 3*B*, the decline in initial current has roughly the same time course as that of a mini. The implication of this is that minis are more or less synchronous initially, whereas later they are not.

DISCUSSION

Several different models of transmitter release are compatible with the kinetics reported here. One interpretation would be that initial synchronous release of vesicles was a mode of release entirely separate from slower subsequent release. Such

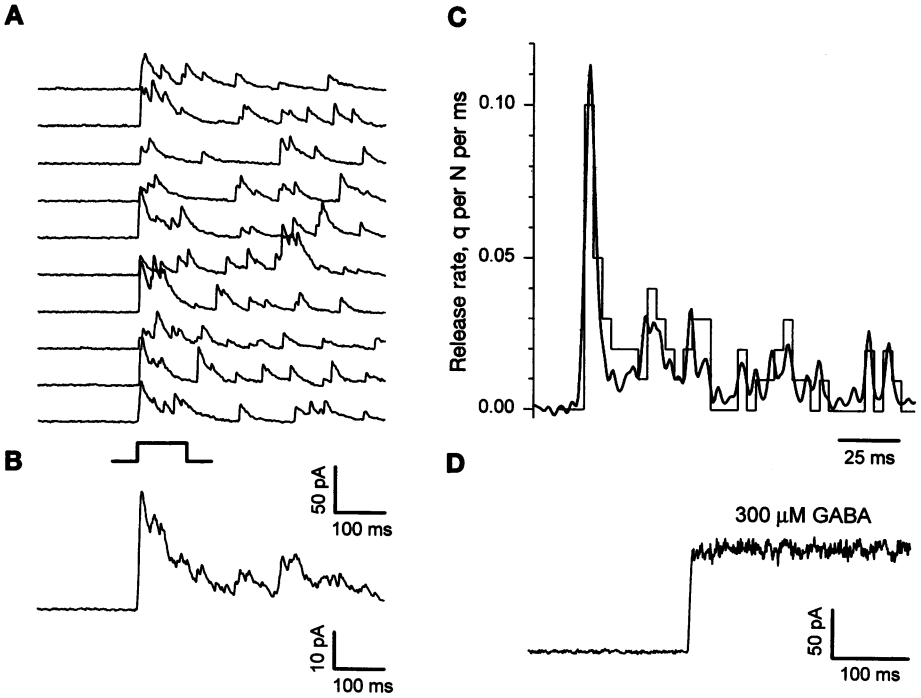

FIG. 3. Desensitization does not account for the form of the release rate function. (*A*) Postsynaptic current records from 10 iterations of a 100-ms presynaptic step to 0 mV. Individual minis may be resolved in these records since exhaustion had diminished the number of functional release sites. N was estimated to be 2.63 and p was 1.07. The mean evoked current shown in *B* is qualitatively similar to those determined for unexhausted cells (e.g., Fig. 2*B*). By using the data shown in *A*, the onsets of minis have been identified from peaks in the time derivative of the current records. Binning these start times produced the histogram shown in *C* that represents an estimate of the release rate, independent of the deconvolution method (the smooth function in *C*). The good agreement between the two methods implies that changes in mini amplitude cannot account for the apparent decrease in release rate. q, Quanta; N, number of release sites. (*D*) Current recorded from a single isolated amacrine cell to which 300 μM GABA was rapidly applied from a puff pipet. In this cell, a current increase from 10 to 90% maximum occurred within 5 ms but desensitization with a time constant that would account for the transients of the evoked current was not seen.

a scheme has recently been proposed for hippocampal neurons (32) based on release elicited by action potentials. We cannot rule out this model but to account for our results completely would require of the model that the mechanism of synchronous release be capable of releasing only a single vesicle at each release site prior to an unknown resetting event, such as a drop in Ca^{2+} concentration. An alternative parsimonious scheme that we favor could be called "fire and reload" and is similar to models of release proposed for nonneuronal and neuroendocrine cells (5, 33–35). A small number of primed vesicles, very likely one per release site, can be quickly exocytosed upon the influx of Ca^{2+}. On average, 45 ms is then required before the next vesicle is exocytosed at the release site. Except perhaps for a short time required for actual exocytosis, the wait must be spent in readying the next vesicle. We have called this process "reloading" and it may actually correspond to the physical translocation of a vesicle on a motor protein. Alternatively, a phosphorylation event (36) might be rate limiting.

Recent measurements of release rates at another retinal synapse, a bipolar cell synapse (6, 7), form an interesting comparison with those presented here for amacrine cells. A striking point of difference is that, with Ca^{2+} influx through Ca^{2+} channels, sustained rates of release per release site are an order of magnitude higher than we find. A distinction between initial and sustained rates is not apparent in bipolar cells and may not exist. Bipolar cells, because of their presynaptic ribbons and lack of synapsins (37), may be specialized for high rates of continuous release. The amacrine cells we describe here may represent a more usual kind of synapse with more limited performance.

Whatever the mechanism, the existence of a relatively long reloading time sets an upper frequency limit on the rate at which synapses may be driven. One way around this constraint might be to employ a large number of release sites, each of which has a low probability of releasing a vesicle of transmitter in response to an action potential, in effect buying speed at the expense of redundancy (1). Because of the small Ca^{2+} influx permitted, a value of p substantially less than 1 would be expected for brief action potentials in the amacrine cells described here, as has been reported at other central synapses (38, 39).

We thank Craig Jahr, William Roberts, Paul Thomas, and Robert Zucker for comments on the manuscript and Matt Frerking for useful suggestions. This work was supported by National Eye Institute Grant EY04112 to M.W. and National Science Foundation Grant DEB 91-19463 to M.T.

1. Almers, W. (1994) *Nature (London)* **367,** 682–683.
2. Neher, E. & Marty, A. (1982) *Proc. Natl. Acad. Sci. USA* **79,** 6712–6716.
3. Fernandez, J. M., Neher, E. & Gomperts, B. T. (1984) *Nature (London)* **312,** 453–455.
4. Thomas, P., Surprenant, A. & Almers, W. (1990) *Neuron* **5,** 723–733.
5. Thomas, P., Wong, J. G., Lee, A. K. & Almers, W. (1993) *Neuron* **11,** 93–104.
6. von Gersdorff, H. & Matthews, G. (1994) *Nature (London)* **367,** 735–739.
7. Heidelberger, R., Heinemann, C., Neher, E. & Matthews, G. (1994) *Nature (London)* **371,** 513–515.
8. Rieke, F. & Schwartz, E. A. (1994) *Neuron* **13,** 863–873.
9. Parsons, T. D., Lenzi, D., Almers, W. & Roberts, W. M. (1994) *Neuron* **13,** 875–883.
10. Fatt, P. & Katz, B. (1952) *J. Physiol. (London)* **117,** 109–128.
11. Stevens, C. F. (1993) *Neuron* **10,** 55–63.
12. Bracewell, R. N. (1978) *The Fourier Transform and Its Application* (McGraw-Hill, New York).
13. Dempster, J. (1986) *J. Neurosci. Methods* **18,** 277–285.
14. Van der Kloot, W. (1988) *J. Physiol. (London)* **402,** 595–603.
15. Gleason, E., Borges, S. & Wilson, M. (1993) *J. Neurosci.* **13,** 2359–2370.
16. Gleason, E., Mobbs, P., Nuccitelli, R. & Wilson, M. (1992) *Vis. Neurosci.* **8,** 315–327.
17. Gleason, E., Borges, S. & Wilson, M. (1994) *Neuron* **13,** 1109–1117.
18. Horn, R. & Marty, A. (1988) *J. Gen. Physiol.* **92,** 145–159.
19. Monck, J. R., Robinson, I. M., Escobar, A. L., Vergara, J. L. & Fernandez, J. M. (1994) *Biophys. J.* **67,** 505–514.
20. Roberts, W. M. (1994) *J. Neurosci.* **14,** 3246–3262.
21. Edwards, F. A., Konnerth, A. & Sakmann, B. (1990) *J. Physiol. (London)* **430,** 213–249.
22. Bekkers, J. M., Richerson, G. B. & Stevens, C. F. (1990) *Proc. Natl. Acad. Sci. USA* **87,** 5359–5362.
23. Faber, D. S., Young, W. S., Legendre, P. & Korn, H. (1992) *Science* **258,** 1494–1498.
24. Katz, B. & Miledi, R. (1965) *J. Physiol. (London)* **181,** 656–670.
25. Barrett, E. F. & Stevens, C. F. (1972) *J. Physiol. (London)* **227,** 691–708.
26. Cox, D. R. & Isham, V. (1980) *Point Processes* (Chapman and Hall, London), p. 135.
27. Katz, B. (1969) *The Release of Neural Transmitter Substances* (Liverpool Univ. Press, Liverpool, U.K.).
28. Korn, H. & Faber, D. S. (1991) *Trends Neurosci.* **14,** 439–445.
29. Maconochie, D. J., Zempel, J. M. & Steinbach, J. H. (1994) *Neuron* **12,** 61–71.
30. Celentano, J. J. & Wong, R. K. S. (1994) *Biophys. J.* **66,** 1039–1050.
31. Verdoorn, T. A., Draguhn, A., Ymer, S., Seeburg, P. H. & Sakmann, B. (1990) *Neuron* **4,** 919–928.
32. Goda, Y. & Stevens, C. F. (1994) *Proc. Natl. Acad. Sci. USA* **91,** 12942–12946.
33. Neher, E. & Zucker, R. S. (1993) *Neuron* **10,** 21–30.
34. von Rüden, L. & Neher, E. (1993) *Science* **262,** 1061–1065.
35. Heinemann, C., von Ruden, L., Chow, R. H. & Neher, E. (1993) *Pflügers Arch. Eur. J. Physiol.* **424,** 105–112.
36. Greengard, P., Valtorta, F., Czernik, A. J. & Benfenati, F. (1993) *Science* **259,** 780–785.
37. Mandell, J. W., Townes-Anderson, E., Czernik, A. J., Cameron, R., Greengard, P. & De Camilli, P. (1990) *Neuron* **5,** 19–33.
38. Hessler, N. A., Shirke, A. M. & Malinow, R. (1993) *Nature (London)* **366,** 569–572.
39. Rosenmund, C., Clements, J. D. & Westbrook, G. L. (1993) *Science* **262,** 754–757.